ACCOUNTS
of chemical research

The Electronic Couplings in Electron Transfer and Excitation Energy Transfer

CHAO-PING HSU*

Institute of Chemistry, Academia Sinica, 128 Section 2 Academia Road, Nankang, Taipei 115, Taiwan

RECEIVED ON JUNE 30, 2008

CONSPECTUS

The transport of charge via electrons and the transport of excitation energy via excitons are two processes of fundamental importance in diverse areas of research. Characterization of electron transfer (ET) and excitation energy transfer (EET) rates are essential for a full understanding of, for instance, biological systems (such as respiration and photosynthesis) and opto-electronic devices (which interconvert electric and light energy). In this Account, we examine one of the parameters, the electronic coupling factor, for which reliable values are critical in determining transfer rates. Although ET and EET are different processes, many strategies for calculating the couplings share common themes. We emphasize the similarities in basic assumptions between the computational methods for the ET and EET couplings, examine the differences, and summarize the properties, advantages, and limits of the different computational methods.

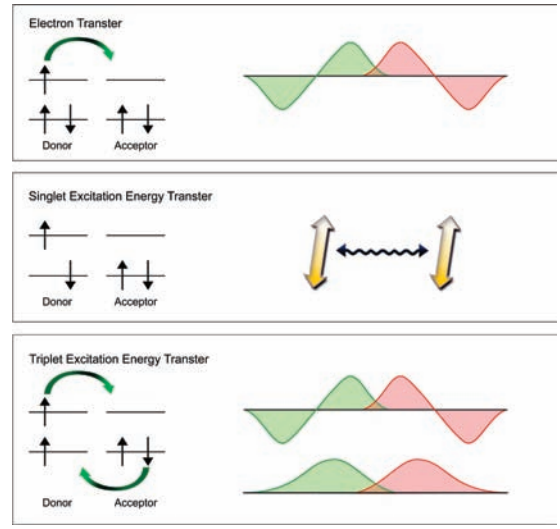

The electronic coupling factor is an off-diagonal Hamiltonian matrix element between the initial and final diabatic states in the transport processes. ET coupling is essentially the interaction of the two molecular orbitals (MOs) where the electron occupancy is changed. Singlet excitation energy transfer (SEET), however, contains a Förster dipole−dipole coupling as its most important constituent. Triplet excitation energy transfer (TEET) involves an exchange of two electrons of different spin and energy; thus, it is like an overlap interaction of two pairs of MOs. Strategies for calculating ET and EET couplings can be classified as (1) energy-gap-based approaches, (2) direct calculation of the off-diagonal matrix elements, or (3) use of an additional operator to describe the extent of charge or excitation localization and to calculate the coupling value.

Some of the difficulties in calculating the couplings were recently resolved. Methods were developed to remove the nondynamical correlation problem from the highly precise coupled cluster models for ET coupling. It is now possible to obtain reliable ET couplings from entry-level excited-state Hamiltonians. A scheme to calculate the EET coupling in a general class of systems, regardless of the contributing terms, was also developed.

In the past, empirically derived parameters were heavily invoked in model description of charge and excitation energy drifts in a solid-state device. Recent advances, including the methods described in this Account, permit the first-principle quantum mechanical characterization of one class of the parameters in such descriptions, enhancing the predictive power and allowing a deeper understanding of the systems involved.

1. Introduction

Transports of charges or excitons are commonly seen fundamental processes in many optoelectronic devices as well as biological systems. The creation, diffusion, and annihilation for excitons and the mobility of charges are some of the key processes in many devices that interconvert electric and light energies.[1,2] Charge transfer is

Published on the Web 02/12/2009 www.pubs.acs.org/acr
10.1021/ar800153f CCC: $71.50

an important process in many biochemical systems, such as those in respiration and photosynthesis.[3,4] The light harvesting and photoprotection in photosynthesis involves singlet and triplet excitation energy transfer (EET).[5] To gain a deep understanding for these systems, it is important to describe the rates of these processes with as few empirically derived parameters as possible.[6,7] Therefore, it has become increasingly important to develop computational techniques that allow us to calculate the rate of charge or energy transport.[8−10]

In a general class of transport processes including electron transfer (ET) and excitation energy transfer (EET), a change in the electronic configuration takes place in a thermally fluctuating environment. In the weak-coupling limit, the rate of both processes can be described by the Fermi golden rule:

$$k_{i\to f} = \frac{2\pi}{\hbar}|V_{if}|^2\delta(E_i - E_f) \tag{1}$$

in which V_{if} is the electronic coupling factor describing the transition between the two electronic states (i and f). Therefore, the rate of such processes can be determined by the density of states and the electronic coupling factor, V_{if}. For example, the Marcus theory[11] and the Förster's rate expression[12] are realizations of such Golden-rule rates for ET and EET, respectively.

The electronic coupling V_{if} is determined by the electronic nature of the molecules or fragments involved. In many works, it is an adjustable parameter determined empirically by a complete measurement and fitting the data to theoretical expressions.[13,14,15] On the other hand, the Condon's approximation[16] allows us to calculate such a coupling for the system without using highly precise models, since the external coordinates, such as the solvent configuration or many vibrational degrees of freedom, generally do not affect the electronic coupling much.[17] Therefore, the electronic coupling is a suitable target for quantum chemistry computation.

A number of computational schemes are available for the ET and EET couplings.[18,19] Despite the different natures in ET and EET couplings, many computational strategies for ET and EET couplings share common themes. In this Account, we discuss the advantages, limits, and general properties of these schemes with an emphasis on their similarities in basic assumptions. In the following sections, we describe computational methods for the ET coupling first. The schemes for both the singlet and triplet EET (SEET and TEET) couplings are included in section 3.

2. Calculating the ET Coupling

In the weak-coupling limit, the ET rate can be described by the Marcus theory[20,21]

$$k_{ET} = \frac{2\pi}{\hbar}|V_{if}|^2\frac{1}{\sqrt{4\pi\lambda k_B T}}\exp\ -\ (\Delta G^\circ + \lambda)^2/(4\lambda k_B T) \tag{2}$$

where λ is the reorganization energy and ΔG° is the standard Gibbs free energy change. Similar to eq 1, the ET rate is proportional to the electronic coupling amplitude squared.

To calculate the electronic coupling factor, a two-state model is often employed, which is composed of the initial and final states of the system. In the two-state model, the Hamiltonian can be written in two different representations:

$$\begin{matrix}\text{charge-localized}\\ \text{states}\end{matrix}\quad \text{eigenstates}$$
$$\begin{pmatrix} E_i & H_{if} \\ H_{if} & E_f \end{pmatrix} \Leftrightarrow \begin{pmatrix} E_1 & 0 \\ 0 & E_2 \end{pmatrix} \tag{3}$$

with the eigenvalues

$$E_{1,2} = \frac{E_i + E_f}{2} \pm \sqrt{\left(\frac{E_i - E_f}{2}\right)^2 + {H_{if}}^2} \tag{4}$$

In the transition state, a resonant situation, $E_i = E_f$, is satisfied. The energy gap becomes

$$|E_1 - E_2| = 2|H_{if}| \tag{5}$$

The overlap matrix element, S_{if}, can be included for more general situations. An effective Hamiltonian can be obtained by the Löwdin symmetric transformation with the off-diagonal element

$$V_{if} \equiv H_{if}^{eff} = \frac{H_{if} - (E_i + E_f)S_{if}/2}{1 - {S_{if}}^2} \tag{6}$$

Under resonance conditions, the energy gap is again twice the effective coupling value:

$$|E_1 - E_2| = 2|V_{if}| \tag{7}$$

The common strategies for calculating electronic coupling factors are listed below with their detailed discussions included in the following sections:

Energy gap, calculating the eigenstate energies, E_1 and E_2, at a resonance condition in which $E_i = E_f$. The coupling values are given by half energy gaps (eq 7).

Direct coupling, treating the states from quantum calculation as charge-localized states and calculating the off-diagonal Hamiltonian, H_{if}, and overlap, S_{if}, directly. For coupling values, eq 6.[22,23]

Use additional operators, using a dipole or charge difference operator to define the charge-localized states. The coupling is then obtained by transforming the two-state Hamiltonian accordingly.[24,25]

2.1. Energy-Gap-Based Schemes. 2.1.1. One-Electron Theory. The energy can be derived from a one-electron theory, or it can be many-electron state energies. One-electron energy is based on Koopmans' theorem (KT)[26] with the Hartree−Fock (HF) wavefunctions. With KT, the energy for an ion can be derived from the energy of a corresponding molecular orbital (MO) of the neutral system. So, coupling is one-half of the energy gap of the two highest occupied MOs (HOMOs) or the two lowest unoccupied MOs (LUMOs) of a neutral donor−acceptor complex. Due to its ease and accessibility, HF-KT is widely used.[27,28]

2.1.2. Many-Electron State Energy: Treating the Nondynamical Correlation. In the energy-gap based approach, the small energy difference between symmetric and antisymmetric adiabatic states is directly proportional to the ET coupling. Typically there are pairs of MOs that are near-degenerate because of the weak interaction between the donor and acceptor fragments, and they lead to near-degenerate target configurations (Figure 1). It is necessary to describe these near-degenerate configurations in a balanced manner for good energy gap values.

The spin-flip (SF) scheme is a useful method to calculate the energy gap in ET coupling.[29,30] In SF, a high-spin configuration is used as a reference state, and the desired low-spin configurations are generated as spin-flipping excitations, as depicted in Figure 1. SF offers a simple way to treat the desired target states in a balanced manner, since the active π (or π^*) orbitals have the same occupancy in the reference state. It avoids the problems caused by using one of the target configurations as the reference state, in which one of the active orbitals is often overstablized at the expense of another active orbital, leading to an unbalanced treatment and an overestimated energy gap.[31]

For the energy gap for an ionic radical, the neutral state can be a good reference with the near-degenerate HOMOs and LUMOs treated in a balanced manner. Therefore, to calculate the energy gap for a radical cation in a hole transfer problem (or an anion for electron transfer), it is possible to obtain the state energies using the ionization potential (or electron affinity) equation of motion coupled cluster (IP-EOMCC or EA-EOMCC) types of approach.[32−34]

The IP-, EA-, and SF-based schemes can be used to systematically study the dynamical correlation effect in ET coupling. Such a dynamical correlation effect was further examined in ET through many-electron bridges as shown in Figure 2.[35] A difference in two symmetry-adapted coupled cluster singles and doubles (CCSD) ground-state energy (ΔCCSD) was also included. In most cases, a good agreement among different CCSD variants is seen. In some cases such as in Figure 2B,D, there are discrepancies between values among the CCSD values, on the order of 10^{-3} eV. They are similar to those reported in a benchmark comparison with full configuration interaction (FCI).[36] Thus more careful studies are needed for the precise correlation effects in these cases.

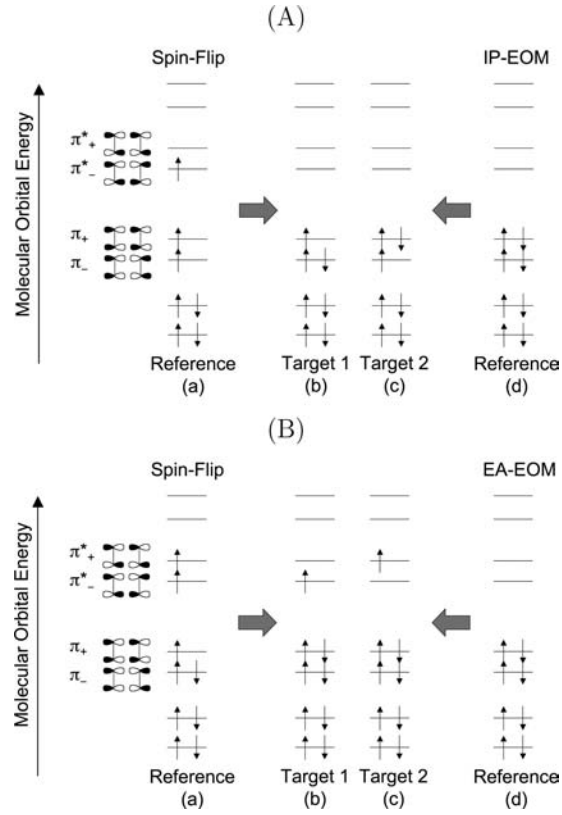

FIGURE 1. Spin-flip (SF), ionization potential (IP), and electron affinity (EA) schemes, with π orbitals depicted for two ethylenes as an example. Shown in panel A) is the scheme for hole transfer (HT) and in panel B that for ET. Configurations in panels a are the charged quartet configuration (for SF) and those in panels d are neutral singlet (IP and EA) reference states. In panels b and c are the target charged, doublet configurations.

2.2. Direct Coupling. The direct coupling (DC) starts with two charge-localizing unrestricted Hartree−Fock (UHF) configurations to mimic the initial and final states $|\Psi_i\rangle$ and $|\Psi_f\rangle$.[38,39] The ET coupling is then calculated via eq 6 with the following elements.[40,41]

$$H_{if} = \langle \Psi_i | \hat{H} | \Psi_f \rangle \tag{8}$$

$$S_{if} = \langle \Psi_i | \Psi_f \rangle \tag{9}$$

DC may not look like a rigorous approach because it assumes that the charge-localized solutions from a quantum computa-

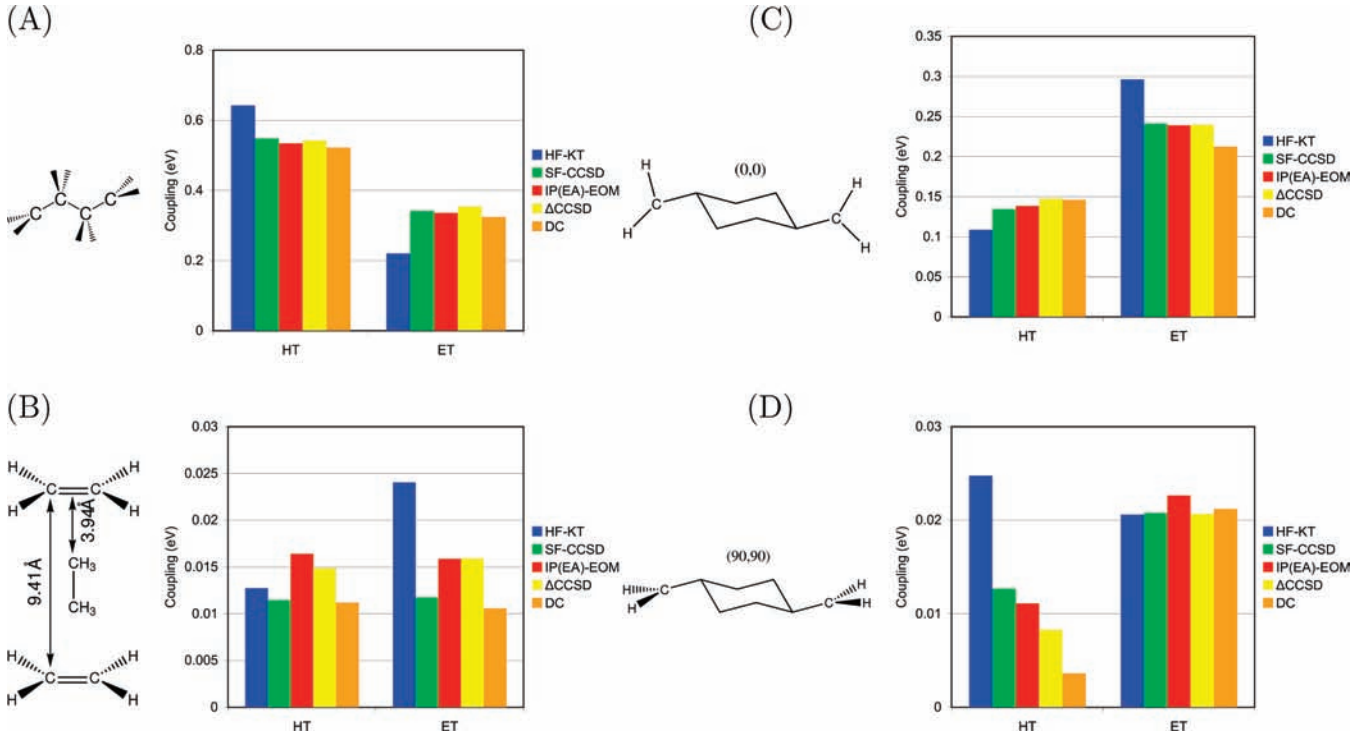

FIGURE 2. Coupling values for both hole transfer (HT) and ET couplings for systems tested.[37]

tion are the diabatic states. However, they have the advantage of low computational cost and generally good results (see Figure 2).[42] In the systems tested, most of the direct coupling (DC) values are very close to those derived from much more expensive CCSD-based schemes.

DC assumes that the two UHF solutions are the two diabatic states, and the eigenstates are assumed to be linear combinations of these two configurations.[43] Therefore, DC uses the approximate dual-configuration solutions as the eigenstates.[44] Including these two configurations is like an approximated multiconfigurational approach for nondynamical correlation. Therefore, DC can be viewed as an inexpensive scheme in which nondynamical correlation is approximately treated.

There are many cases in which the DC and the CCSD results agree well (Figure 2), and the dynamical correlation effect is possibly small in these cases. The relative discrepancies are increased especially for cases with small coupling values (Figure 2B,D). For these systems, we believe a more careful treatment is necessary. ET coupling is usually regarded as a one-electron property with typically small energy values. Electron correlation may add many small terms to it and change the coupling value. The bridge-mediated cases are possible candidates for significant dynamical correlation effects, since the electron is now tunneling through a many-electron environment. From our results, it can be seen that such a possibility exists in some cases, and further study is necessary to address it properly, for example, to compare with couplings derived from other other high-level approaches as possible.[45]

There are simplified variants of DC, which can be used for efficient characterization of ET coupling. One of the them uses the Fock matrix element as the coupling in two donor and acceptor MOs where electron occupancy changes in an ET.[46,47] The relatively low computational cost allows a large number of ET coupling evaluations in simulations. Therefore, such approaches can be seen in many recent works treating charge transporting in organic solids.[48,49] These works are also examples of the emergent works in the literature that connect microscopic electronic structure to the bulk charge transporting properties.

2.3. The Generalized Mulliken−Hush Scheme and Its Variants. Solving the Schrödinger equation yields a set of eigenstates, but the coupling is the Hamiltonian element in a charge-localized space. Generalized Mulliken−Hush (GMH) and its variants use additional operators to define this charge-localized space and calculate the off-diagonal Hamiltonian matrix element. In the first three rows of Table 1, we sketch the operators employed by these schemes in the two different representations, the eigenstates and the charge-localized states, as an introduction.

The GMH scheme is a generalization from the Mulliken−Hush expression, which uses absorption spectra to determine coupling values for optical ET.[50] In GMH,[51] the two

TABLE 1. Schematic Interpretation for GMH, FCD, and FED Methods[a]

transfer	scheme	operator	localized states	eigenstates	coupling (V_{if})
		Hamiltonian	$\begin{pmatrix} E_i & V_{if} \\ V_{if} & E_f \end{pmatrix}$	$\begin{pmatrix} E_1 & 0 \\ 0 & E_2 \end{pmatrix}$	
electron	GMH	diplole	$\begin{pmatrix} \mu_i & 0 \\ 0 & \mu_f \end{pmatrix}$	$\begin{pmatrix} \mu_1 & \mu_{12} \\ \mu_{12} & \mu_2 \end{pmatrix}$	$\frac{\mu_{12}\Delta E_{12}}{\sqrt{(\mu_1-\mu_2)^2+4\mu_{12}^2}}$
electron	FCD	charge difference	$\begin{pmatrix} \Delta q_i & 0 \\ 0 & \Delta q_f \end{pmatrix}$	$\begin{pmatrix} \Delta q_1 & \Delta q_{12} \\ \Delta q_{12} & \Delta q_2 \end{pmatrix}$	$\frac{\Delta q_{12}\Delta E_{12}}{\sqrt{(\Delta q_1-\Delta q_2)^2+4\Delta q_{12}^2}}$
excitation energy	FED	excitation number difference	$\begin{pmatrix} \Delta x_i & 0 \\ 0 & \Delta x_f \end{pmatrix}$	$\begin{pmatrix} \Delta x_1 & \Delta x_{12} \\ \Delta x_{12} & \Delta x_2 \end{pmatrix}$	$\frac{\Delta x_{12}\Delta E_{12}}{\sqrt{(\Delta x_1-\Delta x_2)^2+4\Delta x_{12}^2}}$

[a] Listed are the Hamiltonian and the operators used to find the charge-localized states (or excitation-localized states for FED) in two different representations: the charge- or excitation-localized states and the eigenstates.

charge-localized states are assumed to be the states that have a zero transition dipole moment between them. The ET coupling, V_{if}, is then calculated with two charge-localized states $|i\rangle$ and $|f\rangle$, or in the eigenstate space:

$$V_{if} = \frac{\mu_{12}\Delta E_{12}}{\sqrt{(\mu_1-\mu_2)^2+4\mu_{12}^2}} \tag{10}$$

where μ_{12} is the transition dipole moment, ΔE_{12} is the energy difference, and μ_1 and μ_2 are the permanent dipoles, all of which are calculated between the two eigenstates of the system.

2.3.1. Using a Model Solvent. In photoinduced ET, electron transfer takes place between a locally excited (LE) state and a charge-transfer (CT) state. Since the molecule is modeled in a vacuum, the *ab initio* CT state energy can be very high. A high-energy CT state could couple with other high-lying LE states, leading to an overestimated transition dipole, and thus the final GMH coupling value may become unphysically large.

In a previous work,[52] we found that a simple solvent model, such as the image charge approximation (ICA),[53] can lower the energy of the CT state and decouple it from the undesired high-lying local excitations. We found that coupling strength is weakly dependent on many details of the solvent model, confirming the Condon approximation. Therefore, a trustworthy value can be obtained, with ICA used as a tool to improve and monitor the quality of the results. As seen in Figure 3B, for dimethoxynaphthalene−[polynorbornyl-(8,σ-bonds)]−dicyanovinyl (DMN[8]DCV), one member of a series of well-studied molecules,[54] the GMH coupling value becomes smaller and less dependent on the basis sets when ICA is employed.

2.3.2. The Fragment Charge Difference. The fragment charge difference (FCD) scheme is similar to the GMH. In FCD,[57] a charge difference operator (Table 1) is employed. The molecule is partitioned into two fragments, one for the donor and the other for the acceptor. A 2 × 2 donor−acceptor charge difference matrix, Δq, is defined with its element Δq_{mn}:

$$\Delta q_{mn} = \int_{\mathbf{r}\in D} \rho_{mn}(\mathbf{r})\, d\mathbf{r} - \int_{\mathbf{r}\in A} \rho_{mn}(\mathbf{r})\, d\mathbf{r} \tag{11}$$

where the diagonal elements Δq_{mm} ($\equiv \Delta q_m$) are calculated from the diagonal one-particle density, $\rho_{mm}(\mathbf{r})$, and the off-diagonal Δq_{mn} is the corresponding quantity from the transition density, $\rho_{mn}(\mathbf{r})$,

$$\rho_{mn}(\mathbf{r}) = N\int \ldots \int d\mathbf{r}_2 \ldots d\mathbf{r}_N\, \Psi_m(\mathbf{r}, \mathbf{r}_2, \ldots \mathbf{r}_N)\Psi_n^*(\mathbf{r}, \mathbf{r}_2, \ldots \mathbf{r}_N) \tag{12}$$

where N is the number of electrons in the system. Therefore, the matrix for charge difference can be calculated in eigenstate space.

$$\Delta\mathbf{q} = \begin{pmatrix} \Delta q_1 & \Delta q_{12} \\ \Delta q_{12} & \Delta q_2 \end{pmatrix} \tag{13}$$

In general $\Delta\mathbf{q}$ is not diagonal because transition density may exist between the two eigenstates. The charge-localized states are defined as the linear combination of the eigenstates that diagonalizes $\Delta\mathbf{q}$ or, equivalently, maximizes charge separation. The coupling is obtained after a transformation of the Hamiltonian,

$$V_{if} = \frac{(E_1 - E_2)|\Delta q_{12}|}{\sqrt{(\Delta q_1 - \Delta q_2)^2 + 4\Delta q_{12}{}^2}} \tag{14}$$

The FCD coupling values are mostly similar to GMH in our tests. In Figure 3C, we include FCD coupling values for DMN[8]DCV. Without a model solvent, the FCD coupling value is not as large as that of GMH. This is because a mix of a high-energy LE states does not lead to a large change in the Δq value, which is a desirable property of FCD.

In FCD, a population analysis scheme, such as the Mulliken population analysis,[58] is necessary. It is known that the Mulliken population analysis suffers from several problems, such as the equal dividing the off-diagonal population to two atoms regardless of their electronegativities. However, since the total charges on the two fragments are calculated, the problems arising from dividing between two atoms are typically small in FCD. In Figure 3, we included the FCD coupling with the real-space based Becke's partition,[51] and found that the results are very similar to the ones with the Mulliken population analysis.

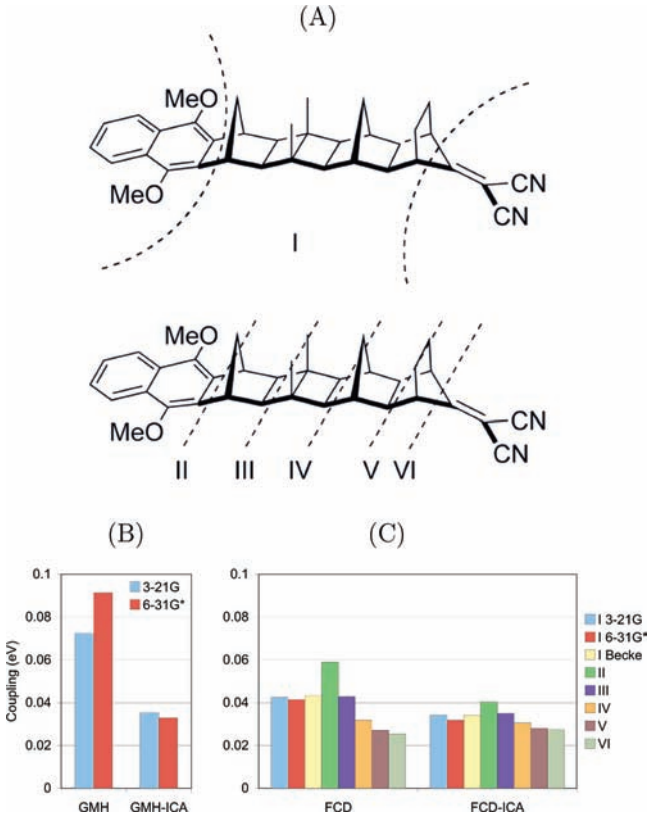

FIGURE 3. A comparison of GMH and FCD coupling values, with and without an ICA model solvent ($\varepsilon = 37.5$), for the molecule shown in panel A. In panel B are the GMH coupling values for two basis sets. In panel C are the FCD coupling values calculated at a number of different partition schemes as shown in panel A. All FCD results were obtained using Mulliken population analysis, except for "I Becke", which was obtained using Becke's partition.[55,56]

For bridge-linked molecules, the donor and acceptor spaces can include bridge fragments for eq 11. In Figure 3, FCD couplings from different partition schemes are included. It is seen that the coupling without including a bridge fragment (I) is similar to those with a piece of bridge, especially when an ICA solvent is employed.

Both GMH and FCD are useful and flexible computational schemes for ET couplings. With entry-level excited-state models, they can be used for large molecules for practical purposes. They can also be used with advanced quantum models for a precise account.[41] The ICA solvent model is a simple way to improve and verify both GMH and FCD results.

3. Excitation Energy Transfer

The electronic excitation energy transfer (EET) is also an important class of transport processes in which the electronic excitation energy is transferred from the donor to the acceptor. The fluorescence resonance energy transfer (FRET) is a widely used technique utilizing EET. The rate of these energy transfer processes can also be described by theories derived from the Fermi golden rule,[23,54]

$$k_{EET} = \frac{2\pi}{\hbar}|V|^2 J \tag{15}$$

where V is the electronic coupling and J is the Franck–Condon factor weighted density of states. The latter is often replaced by the spectral overlap of the donor emission and acceptor absorption spectra.

The most frequently seen EET involves singlet excitation of the fragments. The coupling for such singlet EET (SEET) is a sum of a Coulomb coupling and the short-range coupling.[19,55,57] The former reduces to the Förster dipole–dipole coupling at a large separation,[19] which has an R^{-3} distance dependence, leading to a characteristic R^{-6} dependence for EET *rates*. It is commonly regarded as the dominant interaction in EET. The short-range term consists of Dexter's exchange coupling[55] and an overlap term.[47–49] The former can be regarded as the molecules exchange electrons

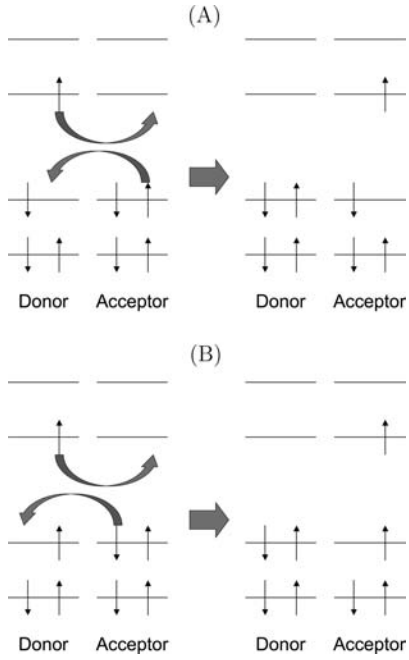

FIGURE 4. Schematic representations for the exchange coupling in singlet (A) and triplet (B) EET.

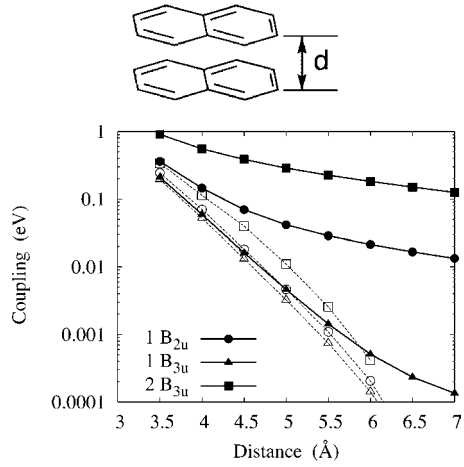

FIGURE 5. FED couplings (closed symbols) and the short-range couplings (corresponding open symbols) for a pair of stacked naphthalenes. The latter were calculated as the difference of FED and Coulomb couplings.

of different energies (Figure 4A). Both contributions have an exponential distance dependence.

There exists another class of EET in which the spin states of the donor and acceptor fragments are changed when energy transfer takes place. In photosynthetic organisms, the triplet chlorophylls (Chls) are inevitable under intense sunlight, and they may convert oxygen to the reactive singlet state through a spin-exchange EET. Carotenoids in photosynthetic proteins can directly quench triplet Chls through a triplet EET (TEET).[8,50] The general rate expression for the TEET process is in the Fermi golden rule framework (eq 15).[54]

Theoretical characterization of TEET coupling has been less frequently seen compared with that for SEET couplings. Earlier works based on semiempirical Hamiltonians reported coupling values that led to orders of magnitudes smaller TEET rates than experimentally observed ones.[50,51] *Ab initio* based methodologies for treating TEET were developed in a more recent work,[52] and the coupling values reported allow a nanosecond TEET rate that is compatible with experimental results.

In this section, we discuss the methods to characterize both TEET and SEET couplings.

3.1. Triplet Excitation Energy Transfer. The TEET starts with the donor in its triplet state, and both the spin and excitation energy are transferred to the acceptor. It can be viewed as two simultaneous electron exchanges with different spin (Figure 4B). It is similar to the Dexter exchange coupling in the SEET[55] (Figure 4A).

In a TEET, the initial and final states are spin-localized states at the donor and acceptor fragments, respectively. The methods used in most of the works seen up until now can be divided into two classes as listed below.

3.1.1. Energy-Gap-Based Scheme. The energy gap of the two triplet states of a donor−acceptor complex can be calculated as excitations (such as configuration interaction singles (CIS)) from a singlet reference, again to avoid unbalanced treatment of orbitals. The energy-gap-based scheme is often used in symmetric systems,[52,54] which naturally satisfy the resonance condition.

For asymmetric systems, it is necessary to manipulate the states to reach resonance, typically by tuning an external parameter continuously, such as a reaction coordinate.[52] We note that for large systems the coordinate scanning may become computationally intensive. It may fail if the triplet state in one of the fragments is highly stabilized over the other fragment because crossing point of the potential energy curves may be hard to find.

3.1.2. Direct Coupling. The second approach was to directly calculate the off-diagonal Hamiltonian matrix element for two spin-localized states.

In many earlier works, a semiempirical Hamiltonian was used to obtain the active MOs. The exchange coupling was calculated by an explicit exchange integral.[51,55,56] In a more recent work,[52] an *ab initio* direct coupling (DC) scheme was used where the off-diagonal Hamiltonian matrix elements are calculated directly,[29] with the initial and final states as spin-localized UHF solutions. In this way, the many-electron effects, such as the relaxation of inactive orbitals, can be fully taken into account.

Despite the many desirable features, such as low computational cost and consistence with CIS energy gaps, DC is not generally applicable to large systems. In the DC approach, it is necessary to start from two UHF configurations, one with triplet donor and the other with triplet acceptor. We note that it is not always possible to obtain these spin-localized configurations.

3.2. Singlet Excitation Energy Transfer. For singlet excitation energy transfer (SEET), both the energy-gap-based approach and directly calculating the Coulomb coupling were seen previously.

3.2.1. Energy-Gap-Based Scheme. The energy-gap-based approach (eq 5) can be used for symmetric systems.[54,57] For a symmetric system with identical donor and acceptor fragments, the resonance condition can be easily satisfied. Since this approach uses eigenvalue difference, it yields the overall couplings. However, like in the TEET case, it is hard to fine-tune the energy levels, making it difficult to study asymmetric systems.

3.2.2. Direct Calculation of the Coulomb Coupling. The "direct coupling" type of calculation in SEET is different from those for ET and TEET. Since Coulomb coupling dominates the SEET coupling and the formalism of the Coulomb coupling in EET is similar to that for electrostatic energy, the coupling is calculated following the dipole, multipole,[58] or full Coulomb interaction[58−51] between the donor and acceptor transitions. The Coulomb integration is

$$J_{coul} = \int d\mathbf{r} \int d\mathbf{r}' \rho_D^*(\mathbf{r}) \frac{1}{|\mathbf{r} - \mathbf{r}'|} \rho_A(\mathbf{r}') \qquad (16)$$

where $\rho_{D(A)}(\mathbf{r})$ is the donor (acceptor) transition density (eq 12). With multipole expansion, the Coulomb interaction (J_{coul}) can be reduced to a sum of a Förster's dipole−dipole coupling, and the higher multipole terms. We note that the multipole expansion that two separated spheres can be drawn, with each enclosing the transition density of a one fragment. In practice, many systems suffer from the validity of multipole expansion.[50] In these cases, it is important to calculate the full Coulomb interaction instead of expanding to higher multipoles.

3.3. Generalizing FCD for EET Couplings. It is possible to generalize the FCD to calculate the EET coupling. In EET, the excitations in eigenstates are usually slightly delocalized. The extent of such delocalization, plus the eigenenergy difference, can in principle determine the EET coupling.

An excitation creates an electron−hole pair. The density of such an electron and a hole can be represented by the attachment and detachment densities, the positive and negative definite parts, respectively, of the difference of the ground- and excited-state densities.[54] Thus we can define the excitation density as the sum of the attachment and detachment densities.

$$\rho_{ex}^{(mn)}(\mathbf{r}) \equiv \rho_{hole}^{(mn)}(\mathbf{r}) + \rho_{elec}^{(mn)}(\mathbf{r}) \qquad (17)$$

where $\rho_{elec}^{(mn)}(\mathbf{r})$ and $\rho_{hole}^{(mn)}(\mathbf{r})$ are the electron (attachment) and hole (detachment) densities created in an excitation.[51,54]

The operator for EET corresponding to the difference in charge, Δq_{mn}, in FCD is

$$\Delta x_{mn} = \int_{\mathbf{r}\in D} \rho_{ex}^{(mn)}(\mathbf{r})\, d\mathbf{r} - \int_{\mathbf{r}\in A} \rho_{ex}^{(mn)}(\mathbf{r})\, d\mathbf{r} \qquad (18)$$

which is the difference in the excitation population. The excitation-localized states are, similar to the charge-localized states, states that have zero off-diagonal excitation difference (Table 1). Following similarly to FCD, the EET coupling can now be evaluated in the excitation localized states as

TABLE 2. A Summary of the Methodologies for ET and EET Couplings

scheme	required computation	advantages	limits
direct coupling	must obtain charge- or spin-localized states for ET and TEET, respectively; for SEET, need excitations for the separate donor and acceptor fragments	typically yields good quality results with a low computational cost; does not need to scan for resonance	mainly for ground-state couplings (ET and TEET); may be hard to find charge- or spin-localized states; hard to justify the assumption of treating calculated states obtained as diabatic states
energy gap	requires the two state energies for the full system; need to scan for the transition state if the system is not symmetric	generally good quality results; based on eigenstate properties	relatively high computational cost; need a proper choice of the reference state to avoid unbalanced treatment in the MOs and overestimating energy gap; for asymmetric systems, scanning for the resonance condition may be expensive, and it may not work for all cases
use additional operators	vertical excitation for the full donor−(bridge)−acceptor system is required; need matrix elements of dipole (GMH), charge difference (FCD) or excitation difference (FED)	suitable for general asymmetric systems; generally good quality results; based on eigenstate properties; does not need to scan for resonance	relatively high computational cost

$$V_{if} = \frac{(E_1 - E_2)|\Delta x_{12}|}{\sqrt{(\Delta x_1 - \Delta x_2)^2 + 4\Delta x_{12}{}^2}} \quad (19)$$

in which $\Delta x_m \equiv \Delta x_{mm}$. In the symmetrical limit, the expression in eq 19 becomes one-half of the energy gap ($E_m - E_n$). The expression in eq 19 is the "fragment excitation difference" (FED) scheme.[51] Similar to FCD, it is convenient to use a population analysis for evaluating eq 18, such as the Mulliken population analysis.

The FED scheme gives the total coupling value under the Hamiltonian model employed, regardless of Coulomb or short-range natures. We have used the FED scheme to show that the bridge-mediated effects observed in a series of *ortho*-phenyleneethynylene oligomer spaced dyads are mainly in the Coulomb coupling, and it is a result of the bridge polarizability.[55]

We note that a variant of FED can also be used to characterize TEET coupling. In a typical triplet excitation from a singlet reference, the electron and hole are of opposite spins, and Δx now reflects spin difference in the two fragments. So the similar excitation density can be defined as in eq 18, and the same expression as in eq 19 can be used for the TEET coupling, a scheme we called "fragmented spin difference" (FSD). Similar to FED, FSD yields the total coupling of the Hamiltonian regardless of the physical origin, and it does not require scanning for resonance nor finding any spin-localized solutions, suitable fr many general systems.

3.3.1. The Exchange Coupling in SEET. The exchange nature in SEET was observed in experiments.[56,57] The Dexter's exchange coupling is an exchange integral:

$$J_{ex} = \int d\mathbf{r} \int d\mathbf{r}' \rho_D^*(\mathbf{r}, \mathbf{r}') \frac{1}{|\mathbf{r} - \mathbf{r}'|} \rho_A(\mathbf{r}', \mathbf{r}) \quad (20)$$

where $\rho_{D(A)}(\mathbf{r}',\mathbf{r})$ is the donor (acceptor) transition density matrix. Evaluations of such exchange interaction are seen in works using parametrized Hamiltonians[51] or hydrogen-like orbitals.[56] In addition to the exchange interaction, the charge-transfer configurations also contribute to EET couplings.[58,58]

We have characterized the short-range coupling by taking the difference between the FED and Coulomb couplings.[51] The EET couplings in the first three states of two naphthalenes behave very differently, mainly due to the differences in the transition dipoles (Figure 5), but the curves for short-range couplings are much closer, which indicates a similar exchange interaction in these transitions. Since the full coupling under the CIS Hamiltonian for the dimer is accounted, the possible charge-transfer configuration effects, as well as any other overlap effects, are included implicitly in our approach.

4. Summary

In Table 2, we summarize the major properties in the three classes of computational methods. In most cases, reliable coupling values can be obtained as long as proper care is taken to avoid problems in the states from which coupling values are derived.

The *ab initio* electronic coupling values offer insights and draw limits to the transport theories. With them it is possible to simulate the charge and exciton transportation with fewer empirical parameters, enhancing the predictive power of computer simulations, and allowing a tight connection from microscopic description to macroscopic properties. Better understanding on the structural and functional designs of molecules and on their device performance can be drawn, which can be used to make further progresses.

We are grateful for the support from the National Science Council and Academia Sinica. The author thanks Zhi-Qiang You for his help with the data presented.

BIOGRAPHICAL INFORMATION

Chao-Ping Hsu was born in Taiwan in 1968. She received a Ph.D. in Chemistry in 1998 from the California Institute of Technology. She was a Miller Research Fellow at the University of California at Berkeley from 1998 to 2001. She joined the Institute of Chemistry, Academia Sinica, in 2002, where she is now an associate research fellow. Her main research interest in computational chemistry has been in the characterization of electronic coupling for charge and energy transports.

FOOTNOTES

*E-mail: cherri@sinica.edu.tw.

REFERENCES

1 Spanggaard, H.; Krebs, F. C. A Brief History of the Development of Organic and Polymeric Photovoltaics. *Sol. Energy Mater. Sol. Cells* **2004**, *83*, 125–146.
2 Shirota, Y.; Kageyama, H. Charge Carrier Transporting Molecular Materials and Their Applications in Devices. *Chem. Rev.* **2007**, *107*, 953–1010.
3 Gray, H. B.; Winkler, J. R. Electron Tunneling through Proteins. *Q. Rev. Biophys.* **2003**, *36*, 341–372.
4 McLendon, G.; Hake, R. Interprotein Electron Transfer. *Chem. Rev.* **1992**, *92*, 481–490.
5 Cogdell, R. J.; Howard, T. D.; Bittl, R.; Schlodder, E.; Geisenheimer, I.; Lubitz, W. How Carotenoids Protect Bacterial Photosynthesis. *Philos. Trans. R. Soc. London, Ser. B* **2000**, *355*, 1345–1349.
6 Bässler, H. Charge Transport in Disordered Organic Photoconductors: A Monte Carlo Simulation Study. *Phys. Status Solidi B* **1993**, *175*, 15–56.
7 Kenkre, V. M.; Andersen, J. D.; Dunlap, D. H.; Duke, C. B. Unified Theory of the Mobilities of Photoinjected Electrons in Naphthalene. *Phys. Rev. Lett.* **1989**, *62*, 1165–1168.
8 Newton, M. D. Quantum Chemical Probes of Electron-Transfer Kinetics: The Nature of Donor−Acceptor Interactions. *Chem. Rev.* **1991**, *91*, 767–792.
9 Bredas, J. L.; Beljonne, D.; Coropceanu, V.; Cornil, J. Charge-Transfer and Energy-Transfer Processes in π-Conjugated Oligomers and Polymers: A Molecular Picture. *Chem. Rev.* **2004**, *104*, 4971–5004.
10 Prytkova, T. R.; Kurnikov, I. V.; Beratan, D. N. Coupling Coherence Distinguishes Structure Sensitivity in Protein Electron Transfer. *Science* **2007**, *315*, 622–625.

11 Marcus, R. A. On the Theory of Oxidation-Reduction Reactions Involving Electron Transfer. I. *J. Chem. Phys.* **1956**, *24*, 966–978.

12 Förster, Th. Zwischenmolekulare Energiewanderung und Fluoreszenz. *Ann. Phys. (Leipzig)* **1948**, *437*, 55–75.

13 Bixon, M.; Jortner, J.; Verhoeven, J. W. Lifetimes for Radiative Charge Recombination in Donor−Acceptor Molecules. *J. Am. Chem. Soc.* **1994**, *116*, 7349–7355.

14 Condon, E. U. Nuclear Motions Associated with Electron Transitions in Diatomic Molecules. *Phys. Rev.* **1928**, *32*, 858–872.

15 In our tests, a change in the structure without directly changing critical parameters such as the donor−acceptor distance led to variations within half of an order of magnitude.

16 Speiser, S. Photophysics and Mechanisms of Intramolecular Electronic Energy Transfer in Bichromophoric Molecular Systems: Solution and Supersonic Jet Studies. *Chem. Rev.* **1996**, *96*, 1953–1976.

17 Hush, N. S. Adiabatic Rate Processes at Electrodes. I. Energy-Charge Relationships. *J. Chem. Phys.* **1958**, *28*, 962–972.

18 Ohta, K.; Closs, G. L.; Morokuma, K.; Green, N. J. Stereoelectronic Effects in Intramolecular Long-Distance Electron Transfer in Radical Anions As Predicted by ab Initio MO Calculations. *J. Am. Chem. Soc.* **1986**, *108*, 1319–1320.

19 Zhang, L. Y.; Friesner, R. A.; Murphy, R. B. *Ab Initio* Quantum Chemical Calculation of Electron Transfer Matrix Elements for Large Molecules. *J. Chem. Phys.* **1997**, *107*, 450–459.

20 Cave, R. J.; Newton, M. D. Generalization of the Mulliken-Hush Treatment for the Calculation of Electron Transfer Matrix Elements. *Chem. Phys. Lett.* **1996**, *249*, 15–19.

21 Voityuk, A. A.; Rösch, N. Fragment Charge Difference Method for Estimating Donor−Acceptor Electronic Coupling: Application to DNA π-Stacks. *J. Chem. Phys.* **2002**, *117*, 5607–5616.

22 Koopmans, T. Über die Zuordnung von Wellenfunktionen und Eigenwerten zu den Einzelnen Elektronen Eines Atoms. *Physica* **1934**, *1*, 104–113.

23 Liang, C.; Newton, M. D. Ab Initio Studies of Electron Transfer: Pathway Analysis of Eective Transfer Integrals. *J. Phys. Chem.* **1992**, *96*, 2855–2866.

24 Lin, B. C.; Cheng, C. P.; You, Z.-Q.; Hsu, C.-P. Charge Transport Properties of Tris(8-hydroxyquinolinato)aluminum(III): Why It Is an Electron Transporter. *J. Am. Chem. Soc.* **2005**, *127*, 66–67.

25 Krylov, A. I. Spin-Flip Equation-of-Motion Coupled-Cluster Electronic Structure Method for a Description of Excited States, Bond Breaking, Diradicals, and Triradicals. *Acc. Chem. Res.* **2006**, *39*, 83–91.

26 You, Z.-Q.; Shao, Y.; Hsu, C.-P. Calculating Electron Transfer Couplings by the Spin-Flip Approach: Energy Splitting and Dynamical Correlation Effects. *Chem. Phys. Lett.* **2004**, *390*, 116–123.

27 Stanton, J. F.; Gauss, J. Analytic Energy Derivatives for Ionized States Described by the Equation-of-Motion Coupled Cluster Method. *J. Chem. Phys.* **1994**, *101*, 8938–8944.

28 Yang, C.-H.; Hsu, C.-P. The Dynamical Correlation in Spacer-Mediated Electron Transfer Couplings. *J. Chem. Phys.* **2006**, *124*, 244507.

29 Pieniazek, P. A.; Arnstein, S. A.; Bradforth, S. E.; Krylov, A. I.; Sherrill, C. D. Benchmark Full Configuration Interaction and Equation-of-Motion Coupled-Cluster Model with Single and Double Substitutions for Ionized Systems Results for Prototypical Charge Transfer Systems: Noncovalent Ionized Dimers. *J. Chem. Phys.* **2007**, *127*, 164110.

30 All computational results presented are from a developmental version of Q-Chem: Shao, Y. Advances in Methods and Algorithms in a Modern Quantum Chemistry Program Package. *Phys. Chem. Chem. Phys.* **2006**, *8*, 3172–3191.

31 Braga, M.; Larsson, S. Correlation Effects in the Electronic Coupling between Electrons through a Cyclohexane Spacer. *Chem. Phys. Lett.* **1992**, *200*, 573–579.

32 Troisi, A. Prediction of the Absolute Charge Mobility of Molecular Semiconductors: The Case of Rubrene. *Adv. Mater.* **2007**, *19*, 2000–2004.

33 Kwiatkowski, J. J.; Nelson, J.; Li, H.; Bredas, J. L.; Wenzel, W.; Lennatz, C. Simulating Charge Transport in Tris(8-hydroxyquinoline) Aluminium. *Phys. Chem. Chem. Phys.* **2008**, *10*, 1852–1858.

34 Hush, N. S. Homogeneous and heterogeneous optical and thermal electron transf. *Electrochim. Acta* **1968**, *13*, 1005–1023.

35 Chen, H.-C.; Hsu, C.-P. Ab Initio Characterization of Electron Transfer Coupling in Photoinduced Systems: Generalized Mulliken−Hush with Conguration-Interaction Singles. *J. Phys. Chem. A* **2005**, *109*, 11989–11995.

36 Friedman, H. L. Image Approximation to the Reaction Field. *Mol. Phys.* **1975**, *29*, 1533–1543.

37 Oevering, H.; Paddon-Row, M. N.; Heppener, H.; Oliver, A. M.; Cotaaris, E.; Verhoeven, J. W.; Hush, N. S. Long-Range Photoinduced Through-Bond Electron Transfer and Radiative Recombination via Rigid Nonconjugated Bridges: Distance and Solvent Dependence. *J. Am. Chem. Soc.* **1987**, *109*, 3258–3269.

38 Becke, A. D. A Multicenter Numerical Integration Scheme for Polyatomic Molecules. *J. Chem. Phys.* **1988**, *88*, 2547–2553.

39 Mulliken, R. S. Electronic Population Analysis on LCAO-MO Molecular Wave Functions. I. *J. Chem. Phys.* **1955**, *23*, 1833–1840.

40 Lin, S. H. On the Theory of Non-Radiative Transfer of Electonic Excitation. *Proc. R. Soc. London, Ser. A* **1973**, *335*, 51–66.

41 Dexter, D. L. A Theory of Sensitized Luminescence in Solids. *J. Chem. Phys.* **1953**, *21*, 836–850.

42 Hsu, C.-P.; Fleming, G. R.; Head-Gordon, M.; Head-Gordon, T. Excitation Energy Transfer in Condensed Media. *J. Chem. Phys.* **2001**, *114*, 3065–3072.

43 Harcourt, R. D.; Scholes, G. D.; Ghiggino, K. P. Rate Expressions for Excitation Transfer. II. Electronic Considerations of Direct and Through-Configuration Exciton Resonance Interactions. *J. Chem. Phys.* **1994**, *101*, 10521–10525.

44 Scholes, G. D.; Ghiggino, K. P. Electronic Interactions and Interchromophore Excitation Transfer. *J. Phys. Chem.* **1994**, *98*, 4580–4590.

45 Rondonuwu, F. S.; Taguchi, T.; Fujii, R.; Yokoyama, K.; Koyama, Y.; Watanabe, Y. The Energies and Kinetics of Triplet Carotenoids in the Lh2 Antenna Complexes as Determined by Phosphorescence Spectroscopy. *Chem. Phys. Lett.* **2004**, *384*, 364–371.

46 Damjanovic, A.; Ritz, T.; Schulten, K. Energy Transfer between Carotenoids and Bacteriochlorophylls in Light-Harvesting Complex II of Purple Bacteria. *Phys. Rev. E* **1999**, *59*, 3293–3311.

47 You, Z.-Q.; Hsu, C.-P.; Fleming, G. R. Triplet−Triplet Energy-Transfer Coupling: Theory and Calculation. *J. Chem. Phys.* **2006**, *124*, 044506.

48 Clayton, A. H. A.; Scholes, G. D.; Ghiggino, K. P.; Paddon-Row, M. N. Through-Bond and Through-Space Coupling in Photoinduced Electron and Energy Transfer: An Ab Initio and Semiempirical Study. *J. Phys. Chem.* **1996**, *100*, 10912–10918.

49 Jortner, J.; Choi, S.-I.; Katz, J. L.; Rice, S. A. Triplet Energy Transfer and Tripelt-Triplet Interaction in Aromatic Crystals. *Phys. Rev. Lett.* **1963**, *11*, 323–326.

50 Levy, S.-T.; Speiser, S. Calculation of the Exchange Integral for Short Range Intramolecular Electronic Energy Transfer in Bichromophoric Molecules. *J. Chem. Phys.* **1992**, *96*, 3585–3593.

51 Pettersson, K.; Kyrychenko, A.; Rönnow, E.; Ljungdahl, T.; Mårtensson, J.; Albinsson, B. Singlet Energy Transfer in Porphyrin-Based Donor−Bridge−Acceptor Systems: Interaction between Bridge Length and Bridge Energy. *J. Phys. Chem. A* **2006**, *110*, 310–318.

52 Krueger, B. P.; Scholes, G. D.; Fleming, G. R. Calculation of Couplings and Energy-Transfer Pathways between the Pigments of LH2 by the ab Initio Transition Density Cube Method. *J. Phys. Chem. B* **1998**, *102*, 5378–5386.

53 Hsu, C.-P.; Walla, P. J.; Head-Gordon, M.; Fleming, G. R. The Role of the S1 State of Carotenoids in Photosynthetic Energy Transfer: The Light-Harvesting Complex II of Purple Bacteria. *J. Phys. Chem. B* **2001**, *105*, 11016–11025.

54 Hsu, C.-P.; You, Z.-Q.; Chen, H.-C. Characterization of the Short-Range Couplings in Excitation Energy Transfer. *J. Phys. Chem. C* **2008**, *112*, 1204–1212.

55 Head-Gordon, M.; Grana, A. M.; Maurice, D.; White, C. A. Analysis of Electronic Transitions as the Difference of Electron Attachment and Detachment Densities. *J. Phys. Chem.* **1995**, *99*, 14261–14270.

56 Chen, H.-C.; You, Z.-Q.; Hsu, C.-P. The Mediated Excitation Energy Transfer: Effects of Bridge Polarizability. *J. Chem. Phys.* **2008**, *129*, 084708.

57 Levy, S.-T.; Rubin, M. B.; Speiser, S. Photophysics of Cyclic α-Diketone romatic Ring Bichromophoric Molecules. Structures, Spectra, And Intramolecular Electronic Energy Transfer. *J. Am. Chem. Soc.* **1992**, *114*, 10747–10756.

58 Scholes, G. D.; Ghiggino, K. P.; Oliver, A. M.; Padden-Row, M. N. Through-Space and Through-Bond Effects on Exciton Interactions in Rigidly Linked Dinaphthyl Molecules. *J. Am. Chem. Soc.* **1993**, *115*, 4345–4349.